Journal of Information Systems Engineering and Management
2025, 10(4)
e-ISSN: 2468-4376
https://www.jisem-journal.com/

Research Article

Numerical Investigation of Rigid Zone Evolution in Herschel–Bulkley Fluids Under Unsteady Flow

Messaouda Elalem[1], Farid Messelmi[2], Hadi Taibi[3]
[1]*Ziane Achour University of Djelfa, Faculty of Exact Sciences and Computer Science, Department of Physics, Laboratory of Development in Physiochemistry of Materials and Environment, Algeria, m.elalem@univ-djelfa.dz*
[2]*Ziane Achour University of Djelfa, Faculty of Exact Sciences and Computer Science, Department of Mathematics, Djelfa 17000, Algeria,*
[3]*Ziane Achour University of Djelfa, Faculty of Technology Science, Department of Mechanical Engineering, Algeria*

ARTICLE INFO

Received: 10 Nov 2024
Revised: 25 Dec 2024
Accepted: 22 Jan 2025

ABSTRACT

Understanding and predicting the formation of rigid zones in viscoplastic flows is essential for optimizing the casting and structural performance of fresh concrete. This study investigates the unsteady-state evolution of rigid zones in concrete modeled as a Herschel–Bulkley fluid. A two-dimensional numerical model was developed using the Papanastasiou regularization method and implemented in COMSOL Multiphysics 6.0 to simulate viscoplastic flow within a plate domain. The simulations reveal that rigid zones emerge and expand as the yield stress and consistency coefficient increase, significantly altering the flow behavior. At low yield stress, the material behaves predominantly as a fluid, while higher yield stress and consistency values promote the formation and growth of rigid zones over time. Conversely, increasing the applied pressure reduces rigid zone formation, leading to a more continuous, Power-law-type flow. Mathematical expressions are proposed to predict the rigid zone area and stagnation time based on yield stress, consistency, and pressure. These findings enhance the understanding of viscoplastic flow dynamics and offer practical tools for predicting and controlling rigid zone development in concrete casting processes.

Keywords: pressure, laminar flow, Herschel-Bulkley fluid, non-stationary flow, rigid zones, stagnation time, consistency coefficient

INTRODUCTION

Non-Newtonian fluids play a critical role in various natural and industrial processes, including concrete casting, petroleum transport, printing, painting, mud flow, and polymer processing. They are also encountered in biological contexts such as blood circulation and in daily-use products like toothpaste, cosmetics, and foodstuffs. Unlike Newtonian fluids, their behavior is governed by a nonlinear relationship between shear stress and shear rate [1,2]. Among the different categories of non-Newtonian fluids, viscoplastic fluids occupy a distinct place due to their dual nature: they behave like solids under low stress but transition into flowing fluids once the yield stress threshold is exceeded, as seen in substances like toothpaste [3]. The Herschel–Bulkley model is one of the most widely adopted frameworks for capturing the complex behavior of viscoplastic materials [4], gaining increasing prominence in both theoretical and applied research [5,6]. These materials exhibit rigid-like resistance below the yield limit, maintaining shape without noticeable deformation. However, once the applied stress surpasses this limit, internal restructuring occurs, resulting in fluid-like behavior. During this transition, the apparent viscosity becomes extremely large as the deformation rate approaches zero, presenting significant challenges for numerical modeling. To address this issue, the Papanastasiou regularization technique was introduced [7], which ensures smooth transitions between rigid and flowing zones. Several studies have explored the impact of its parameters particularly the stress growth exponent m, which modulates how closely the model approximates ideal viscoplastic behavior. While some authors [8] suggest ideal behavior as m approaches infinity, others [9] recommend keeping m below 100 to ensure numerical stability and accuracy. In addition to yield stress effects on effective viscosity [10], high particle concentrations in Herschel–Bulkley fluids can lead to pasty behavior and the emergence of rigid zones due to interparticle interactions. Various studies have investigated how flow parameters influence the size and shape of these zones. Mossaz et al. [11,12] examined the role of the Oldroyd number and power-law index, while other researchers [13] focused on the direct

Journal of Information Systems Engineering and Management
2025, 10(4)
e-ISSN: 2468-4376
https://www.jisem-journal.com/

Research Article

relationship between Oldroyd numbers and the formation of unyielded zones. Messelmi [14], through mathematical analysis, demonstrated that an increase in yield stress promotes the expansion of rigid zones, potentially obstructing flow entirely.

This study seeks to examine the formation and evolution of rigid zones during the unsteady flow of a Herschel–Bulkley fluid. It begins by analyzing the influence of yield stress on the time-dependent development of rigid zones, where a predictive expression is proposed to estimate the rigid area as a function of both yield stress and time. It then focuses on analyzing how key the consistency index influences both the growth and stabilization of rigid zones. Special attention is given to establishing predictive relationships for the rigid area and the stagnation time as functions of the consistency index. Additionally, the study investigates how variations in yield stress and inlet pressure affect the dynamics of rigid zone development over time, offering insights into controlling the spatial and temporal extent of these zones for more accurate modeling of viscoplastic flows.

The organization of this paper is as follows: Section 2 outlines the formulation of the studied problem. In Section 3, the governing mathematical equations are detailed along with the regularization parameters adopted in this work. Section 4 covers the validation process of the numerical simulations as well as the mesh sensitivity analysis. Section 5 is dedicated to the presentation and discussion of the results. Finally, the paper ends with concluding remarks.

OBJECTIVES

The objective of this study is to investigate the formation and temporal evolution of rigid zones in fresh concrete flows modeled as a Herschel–Bulkley fluid. Emphasis is placed on understanding how variations in the yield stress influence the initiation and expansion of these zones during flow, and how the consistency index affects their growth and stabilization over time. Numerical simulations are conducted using COMSOL Multiphysics 6.0 in a two-dimensional domain under unsteady-state conditions. The effect of inlet pressure on the viscoplastic response is also analyzed, particularly its role in suppressing rigid zone formation and promoting power-law behavior at higher values. In addition, the study proposes predictive mathematical expressions for estimating the rigid zone area and stagnation time as functions of rheological parameters and pressure. These objectives aim to provide deeper insights into the mechanics of viscoplastic flow and offer practical tools for predicting and optimizing flow behavior in construction and industrial processes.

METHODS

This study focuses on the evolution of rigid zones within an unsteady, laminar, and isothermal flow of a Herschel–Bulkley fluid. In this context, fresh concrete is modeled as a Herschel–Bulkley material characterized by the following rheological parameters [15]: density density of $\rho = 1370\ kg/m^3$, consistency coefficient $k = 2.42\ Pa.s^n$, flow behavior index $n = 0.552$, and a yield stress $\tau_y = 5\ Pa$. The simulation is conducted in a two-dimensional square plate domain, as illustrated in **Figure 1**, using COMSOL Multiphysics 6.0. The flow is driven by an inlet pressure of $p_{in} = 20\ Pa$. Boundary conditions include a no-slip condition on the walls and a zero-velocity assumption at the outlet.

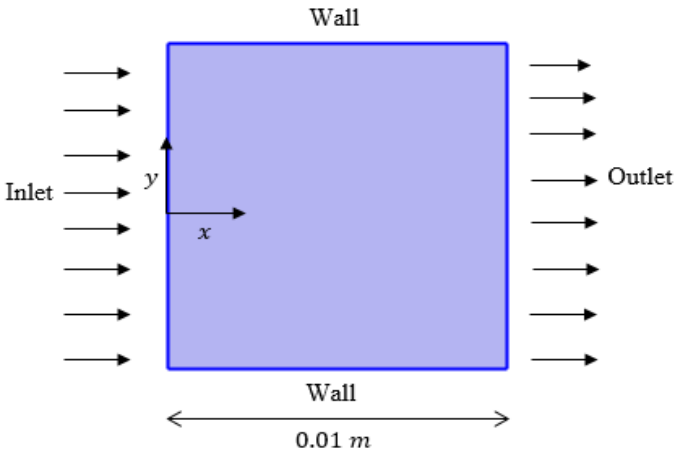

Fig. 1. Geometry of the flow domain.

Journal of Information Systems Engineering and Management
2025, 10(4)
e-ISSN: 2468-4376
https://www.jisem-journal.com/

Research Article

The behavior of the flow is described by the continuity and momentum equations, which are expressed in sequence as follows:

$$\nabla . U = 0 \tag{1}$$

$$\rho \frac{\partial \mathrm{U}}{\partial t} + \rho(\mathrm{U}\nabla)\mathrm{U} = \nabla[-\mathrm{pI} + \tau] + f \tag{2}$$

In the case of a Newtonian fluid, the shear stress is defined by the relation $\tau = 2\mu\dot{\gamma}$, where μ represents the constant viscosity. On the other hand, for a viscoplastic fluid, the shear stress is described by the Herschel–Bulkley (HB) model, formulated as follows [16]:

$$\begin{cases} \tau = (k|\dot{\gamma}|^{n-1} + \frac{\tau_y}{|\dot{\gamma}|})\gamma & \text{if } |\tau| > \tau_y \\ |\dot{\gamma}| = 0 & \text{if } |\tau| \leq \tau_y \end{cases} \tag{3}$$

Where, τ_y is the yield stress, $\dot{\gamma}$ is the shear rate tensor, and $|\dot{\gamma}|$ is its magnitude. The following relations give the shear rate:

$$\dot{\gamma} = \frac{1}{2}[\nabla U + (\nabla U)^T] \tag{4}$$

$$|\dot{\gamma}| = \sqrt{2\ \dot{\gamma} : \dot{\gamma}} \tag{5}$$

According to the Herschel-Bulkley viscoplastic model, the fluid exhibits two different behaviors depending on the level of applied stress. If the stress exceeds the yield threshold, the material flows and behaves in a pseudo-plastic manner. However, when the applied stress is below the yield limit, the fluid does not deform and acts as a rigid solid. In such cases, the apparent viscosity becomes extremely large, tending to infinity as the shear rate approaches zero, i.e., $\lim_{\dot{\gamma}\to 0} \mu(\dot{\gamma}) = \infty$ [17,18]. This behavior leads to the appearance of rigid zones whose size, shape, and location change over time. These zones are mathematically defined by the condition where the shear rate is zero [14].

$$\Omega_r = \{x \in \Omega, \mathrm{t} \geq 0 : |\gamma(U(x.y.t))| = 0\} \tag{6}$$

When the shear rate approaches zero, the constitutive formulation of the Herschel-Bulkley fluid encounters a singularity, which presents significant challenges for numerical modeling. To address this issue, several regularization techniques have been proposed in the literature to smooth out the discontinuity and ensure computational stability [19, 20, 21]. In the present study, the regularization approach proposed by Papanastasiou is employed, leading to a modified form of the Herschel-Bulkley equation as used in previous works [7, 22].

$$\tau = k|\gamma|^{n-1} + \frac{\tau_y}{|\gamma|}[1 - e^{-m|\gamma|}]\gamma \tag{7}$$

and the viscosity takes the formula:

$$\mu(\gamma) = k|\gamma|^{n-1} + \frac{\tau_y}{|\gamma|}[1 - e^{-m|\gamma|}] \tag{8}$$

As previously outlined in the introduction, the regularization parameter m, often referred to as the stress growth exponent, controls how closely the Herschel-Bulkley model approximates the ideal viscoplastic behavior. In this investigation, a value of $m = 10\ s$ is selected. Another key factor in the regularized formulation is the critical shear rate $\dot{\gamma}_c$, which plays a crucial role in determining the extent and position of rigid zones. Drawing on insights from earlier studies, this parameter is set to $\dot{\gamma}_c = 10^{-3}s^{-1}$ [23]. Within this regularization framework, rigid zones are identified as zones where the local shear rate $\gamma^{\cdot}$ is less than or equal to the critical value, i.e.,$\dot{\gamma} \leq \dot{\gamma}_c$ [8]. Consequently,

Journal of Information Systems Engineering and Management
2025, 10(4)
e-ISSN: 2468-4376
https://www.jisem-journal.com/

Research Article

the rigid zones can be mathematically characterized using this criterion.

VALIDATION AND GRID STUDY

Verifying the accuracy of the steady-state solution is essential, as it forms the foundation for simulating time-dependent flows. To ensure its reliability, the velocity field predicted by CFD simulations was assessed against exact analytical solutions derived from theoretical analysis. Let us consider a flow confined within a rectangular domain defined by $\Omega = [0; L] \times [0; H]$, where the fluid moves with a constant horizontal velocity. The dimensionless horizontal velocity component is denoted by $u*$, leading to a velocity field expressed as $U = Vu*(y)\vec{e}x$, where V represents a characteristic velocity. The analytical expression for this type of flow is provided in the following equation (Eq. 10) [24].

$$u^* = \frac{1}{M} f^* \begin{cases} \left(\frac{y_0}{H}\right)^M - \left(\frac{y_0 - y}{H}\right)^M & \text{if } 0 \le y \le y_0 \\ \left(\frac{y_0}{H}\right)^M & \text{if } y_0 \le y \le H - y_0 \\ \left(\frac{y_0}{H}\right)^M - \left(\frac{y - (H - y_0)}{H}\right)^M & \text{if } H - y_0 \le y \le H \end{cases} \tag{10}$$

Where $M = 1 + \frac{1}{n}; f^* = (\frac{fH}{K})^{\frac{1}{n}} \times \frac{H}{V}$ is the non-dimensional gradient force and $y_0 = \frac{H}{2} - \frac{\tau_y}{f}$.

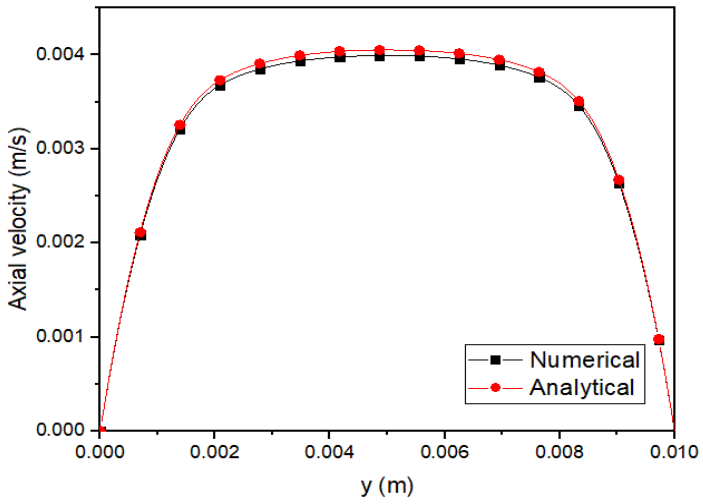

Fig. 2 Comparison of velocity magnitude predicted numerically with the theoretical velocity profiles.

The analytical solution for the horizontal velocity component was compared against the numerical results obtained at the midline $x = H/2$, using COMSOL Multiphysics 6.0. Both profiles are illustrated in **Figure 2**, and the strong agreement between them confirms the validity of the numerical approach employed.

To maintain a high level of accuracy in the simulation, particular attention was given to the mesh design. A structured mapped mesh was utilized, and four different mesh densities were evaluated to identify the most suitable configuration. **Figure 3** presents the axial velocity distribution for the four mesh cases along the direction of flow. The comparison shows a notable convergence between the results from Grid-3 and Grid-4. Consequently, Grid-3 was selected for the entire set of simulations used throughout this study, balancing computational efficiency with reliable numerical precision.

Journal of Information Systems Engineering and Management
2025, 10(4)
e-ISSN: 2468-4376
https://www.jisem-journal.com/

Research Article

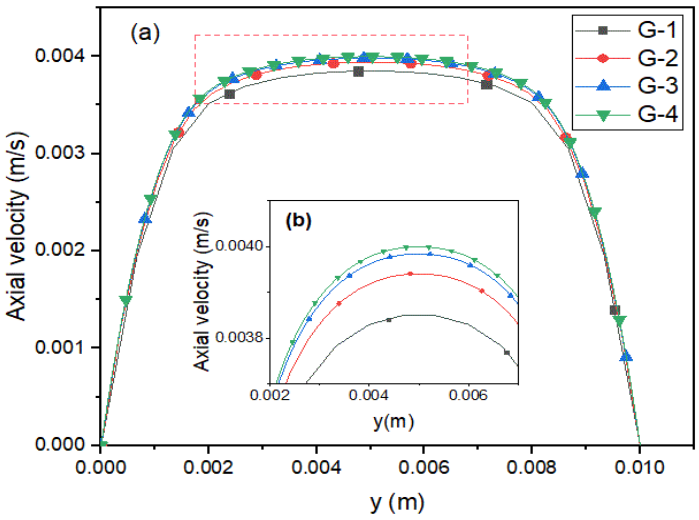

Fig. 3. Axial velocity profiles for different mesh sizes corresponding to Grid-1 (1500 elements), Grid-2 (9750 elements), Grid-3 (10500 elements), and Grid-4 (34034 elements).

RESULTS

EFFECT OF YIELD STRESS ON TEMPORAL GROWTH OF RIGID ZONES

To better understand the temporal evolution of rigid zones under different yield stress conditions, a 3D plot was constructed to visualize the rigid zone area as a function of both time and yield stress.

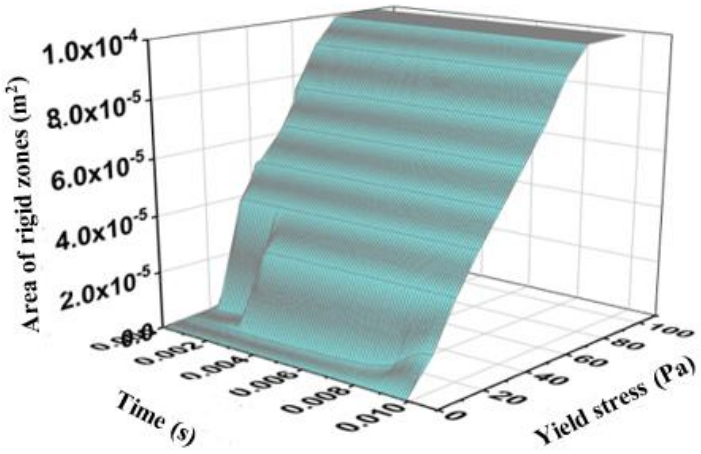

Fig.4. 3D Representation of the evolution of rigid zone area over time for various yield stress values.

Figure 4 presents a three-dimensional surface plot illustrating the evolution of rigid zone areas over time for varying values of yield stress, under conditions where the fresh concrete is already in motion that is, after surpassing its yield stress and entering the flow state. At the initial yield stress of 5 Pa, rigid zones are virtually absent, indicating that the material is fully fluidized and flowing as expected during casting operations. However, as the yield stress is progressively increased, rigid zones begin to emerge within the flowing concrete. This finding is critical: although the material is already in a flowing state, the increase in yield stress causes the formation of rigid-like regions during the flow. These zones not only appear earlier in time with higher yield stress values, but also grow more rapidly and occupy a larger portion of the domain. At a yield stress of approximately 100 Pa, the material approaches near-complete solidification over the studied time window, despite being in a state of flow.

Journal of Information Systems Engineering and Management
2025, 10(4)
e-ISSN: 2468-4376
https://www.jisem-journal.com/

Research Article

To complement the qualitative insights derived from the 3D plot, a linear regression fitting was performed using the simulation data. The resulting empirical model expresses the rigid zone area A_{rigid} as a function of time t and yield stress τ_y :

$$A_{rigid} = z_0 + at + b\tau_y \tag{11}$$

Where z_0, a and b are empirical constants derived from curve fitting.

To further support the trends observed in the 3D plot, **Figure 5** presents a series of visual snapshots illustrating the spatial evolution of rigid zones for various yield stress values. In each case, two key moments were captured: the initial time, when the first signs of solidification appear, and the final time corresponding to the steady-state configuration of the rigid zones.

These visualizations reveal a consistent solidification mechanism: a central rigid nucleus forms near the middle of the flow domain, while another rigid zone simultaneously begins to emerge near the inlet boundary. As time progresses, the central nucleus grows and merges with the rigid zone at the inlet, forming a continuous rigid structure. This process becomes more pronounced with higher yield stress values, aligning with the 3D curve which shows increased rigid zone area over time.

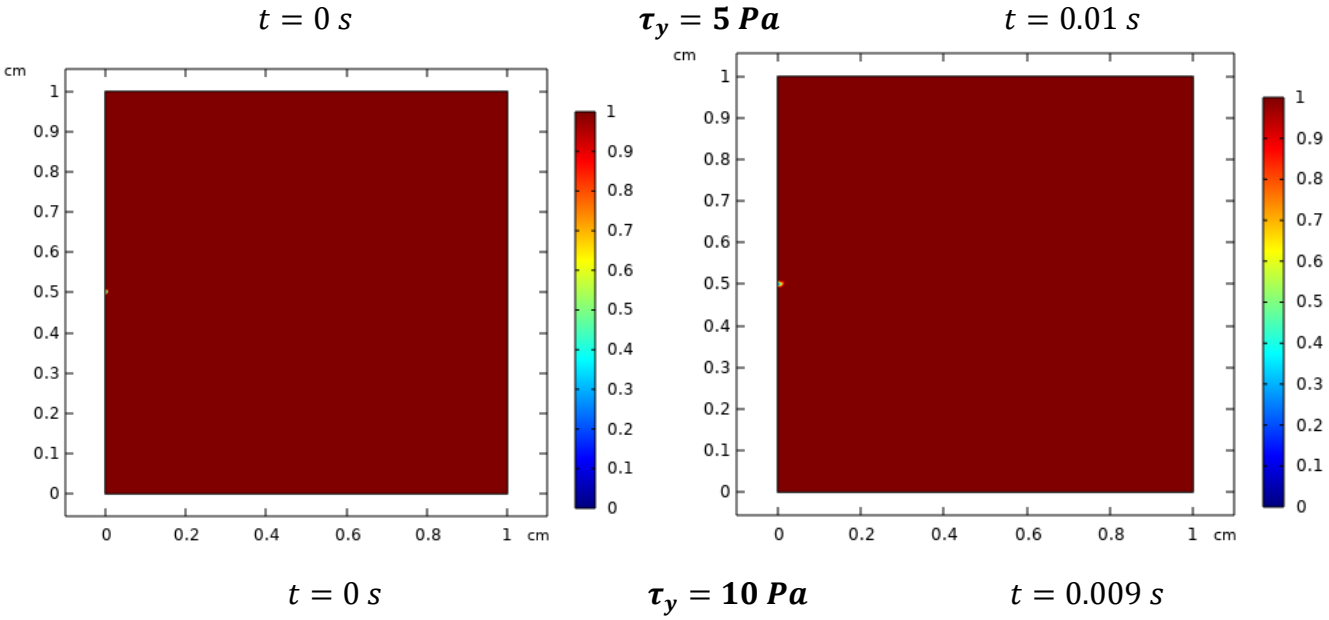

Journal of Information Systems Engineering and Management
2025, 10(4)
e-ISSN: 2468-4376
https://www.jisem-journal.com/

Research Article

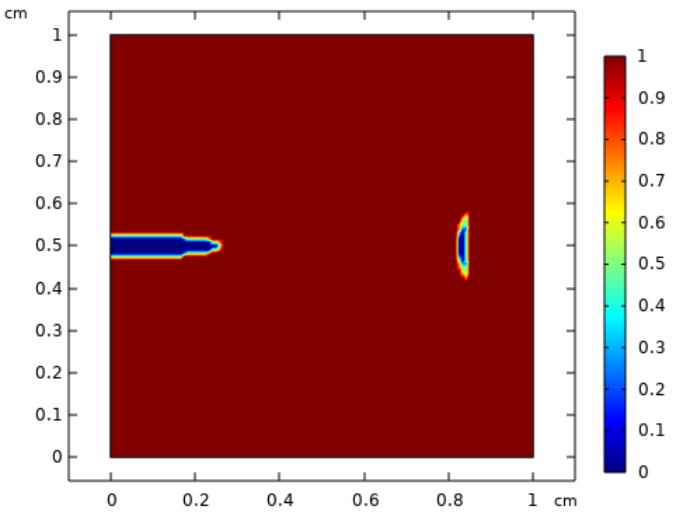

$t = 0\ s$

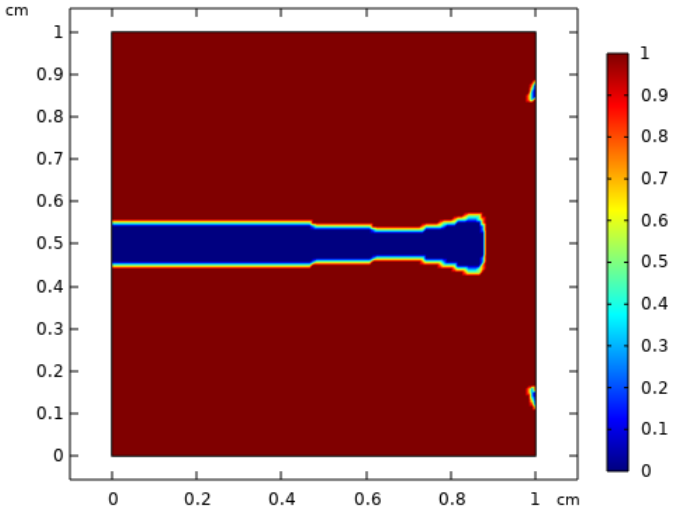

$\boldsymbol{\tau_y = 20\ Pa}$ $t = 0.005\ s$

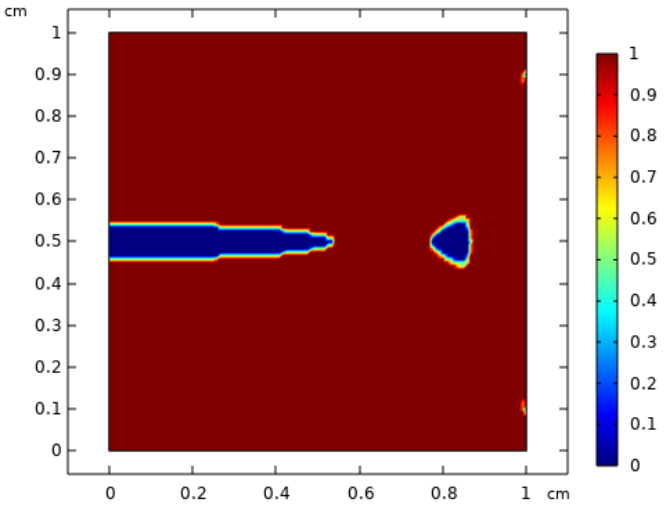

$t = 0\ s$

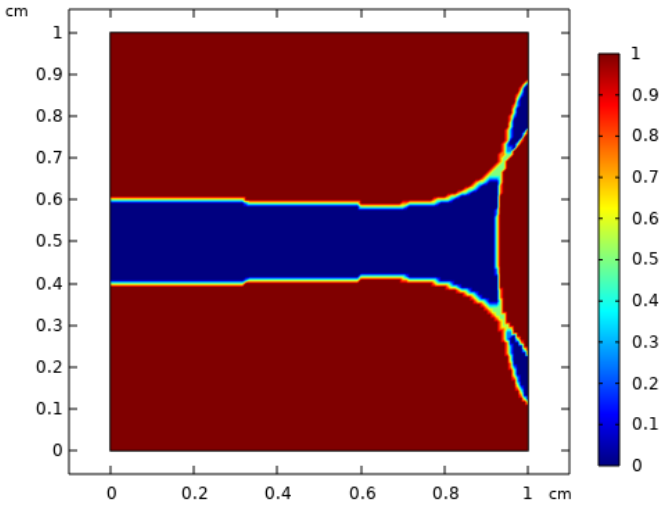

$\boldsymbol{\tau_y = 50\ Pa}$ $t = 0.002\ s$

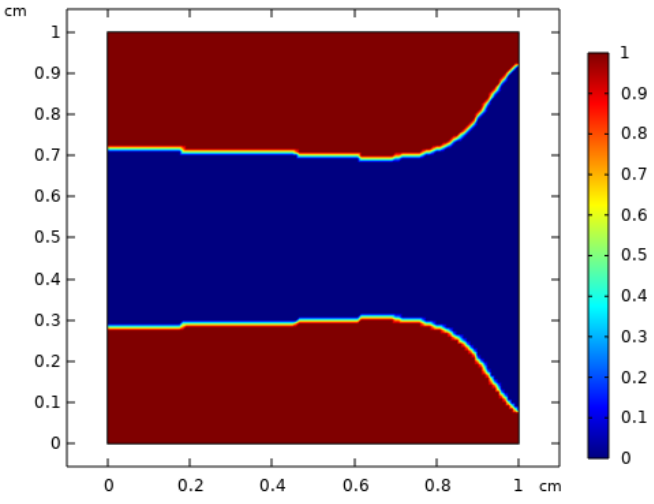

$t = 0\ s$

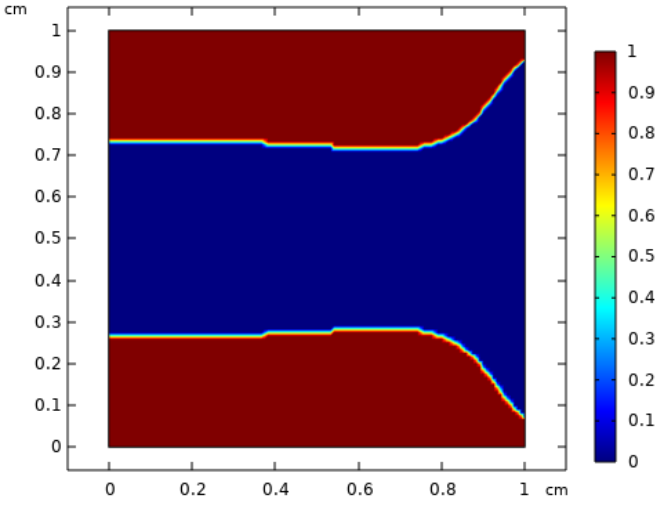

$\boldsymbol{\tau_y = 100\ Pa}$ $t = 0.001\ s$

Journal of Information Systems Engineering and Management
2025, 10(4)
e-ISSN: 2468-4376
https://www.jisem-journal.com/

Research Article

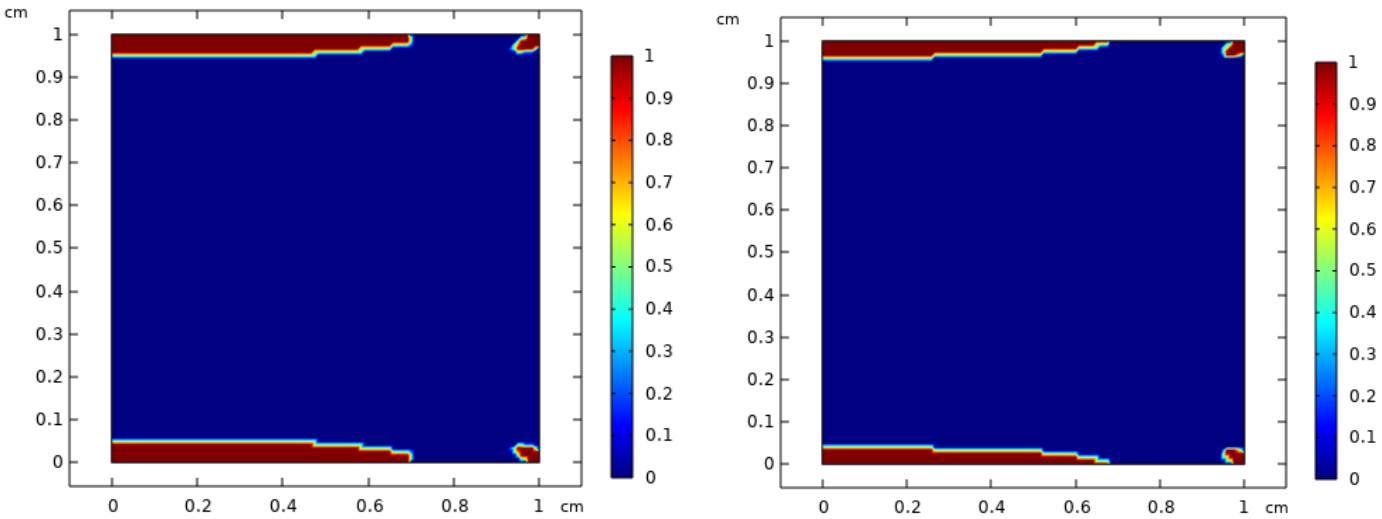

Fig 5. Scenario of rigid zone formation with time for various yield stress values.

INFLUENCE OF CONSISTENCY COEFFICIENT ON THE FORMATION OF RIGID ZONES

To investigate the influence of the material's rheological properties on the formation of rigid zones during flow, the variation of the rigid zones area with respect to the consistency coefficient k was analyzed. The consistency coefficient represents the resistance of the fluid (in this case, fresh concrete) to flow under shear, and its variation is expected to directly affect the flow regime and internal structuring.

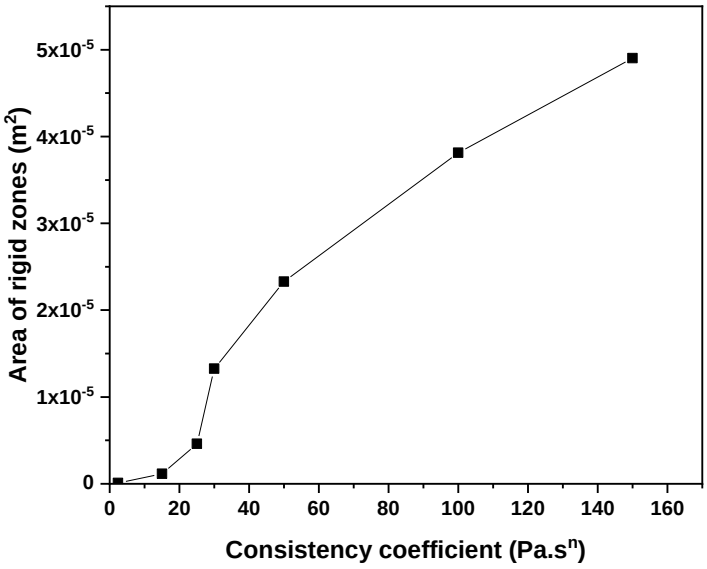

Fig. 6. Evolution of rigid zone area with consistency coefficient at the stagnation point.

The results displayed in **Figure 6** reveal a clear nonlinear increase in the area of rigid zones as the consistency coefficient increases. At low values of K, the area remains negligible, indicating that the fluid maintains its ability to deform and flow homogeneously. However, as k increases beyond a critical threshold (approximately 40 $Pa.s^n$), the area of rigid zones begins to grow significantly. This growth becomes more pronounced at higher values of k, indicating a progressive transition from a fully flowing regime to a partially or even fully stagnant flow configuration. This evolution was quantitatively captured by fitting a mathematical relationship to the data points, leading to the following expression:

Journal of Information Systems Engineering and Management
2025, 10(4)
e-ISSN: 2468-4376
https://www.jisem-journal.com/

Research Article

$$A_{rigid} = aln(-bln(k)) \quad (12)$$

Where a, b are empirical constants derived from curve fitting. The strong correlation between the model and the numerical results confirms the deterministic influence of K on the solidification process.

To support this behavior, **Figure 7** presents the spatial evolution of rigid zones for each studied value of K. These images clearly show how rigid zones initiate at low shear zones primarily near domain boundaries and in flow cores and expand with increasing K.

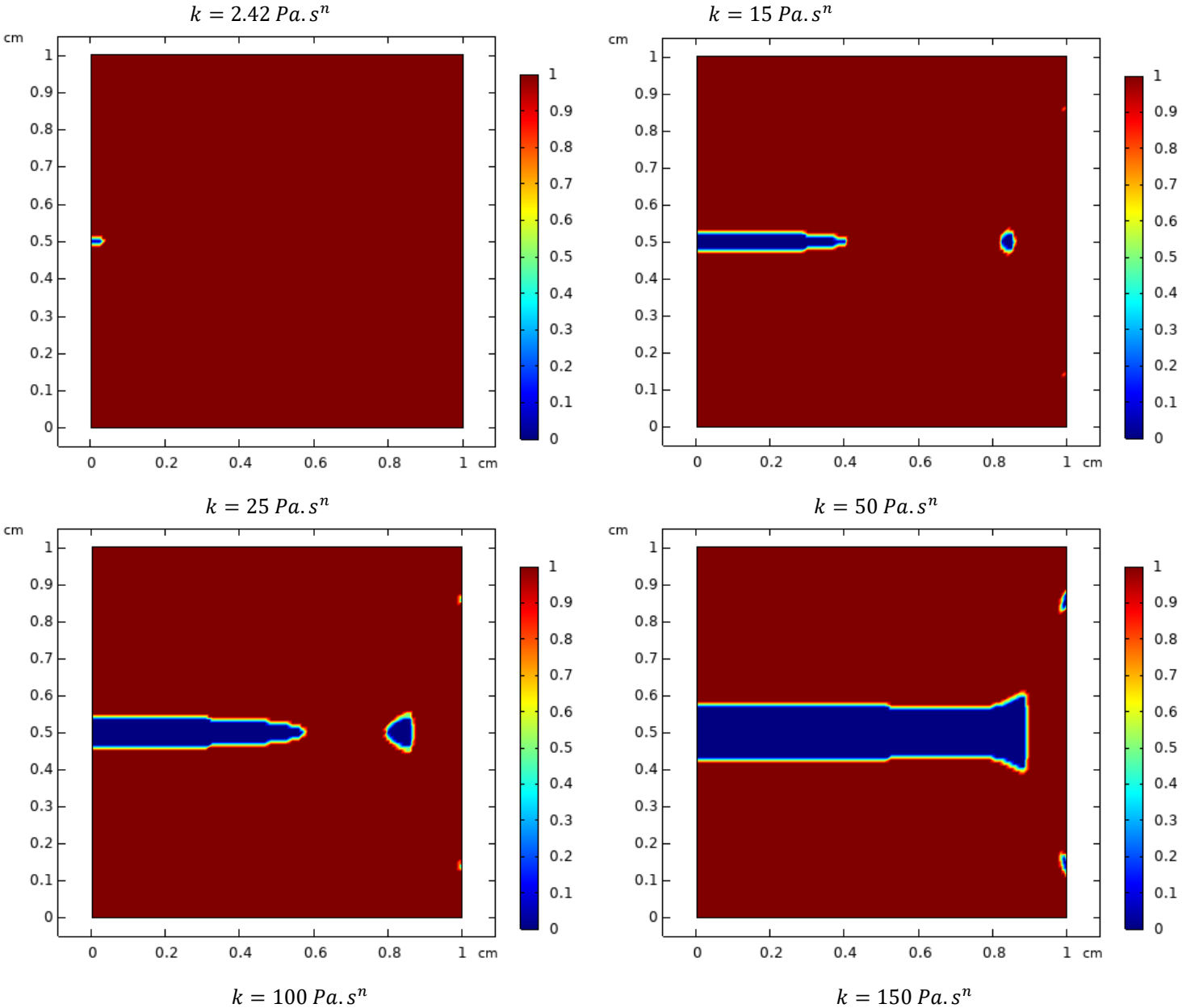

Journal of Information Systems Engineering and Management
2025, 10(4)
e-ISSN: 2468-4376
https://www.jisem-journal.com/

Research Article

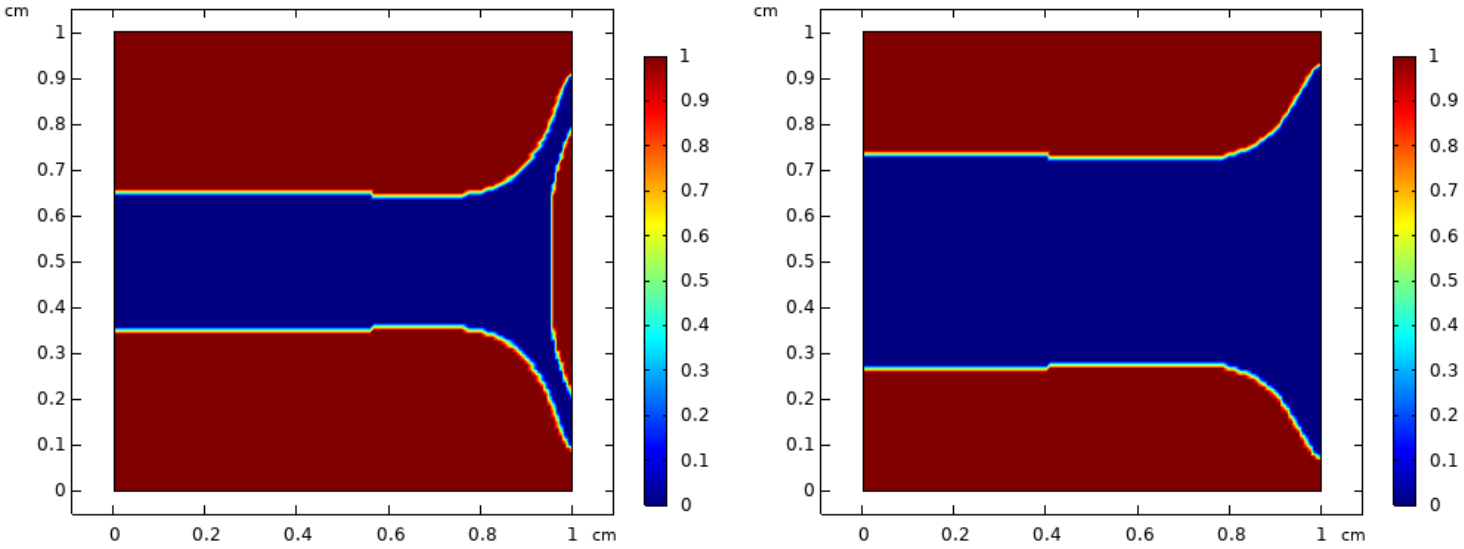

Fig.7. Evolution and localization of rigid zones under varying consistency coefficient.

To gain deeper insight into the evolution of rigid zones in fresh concrete under varying rheological properties, a combined analysis was performed by plotting the stagnation time as a function of both the rigid zone area and the consistency coefficient.

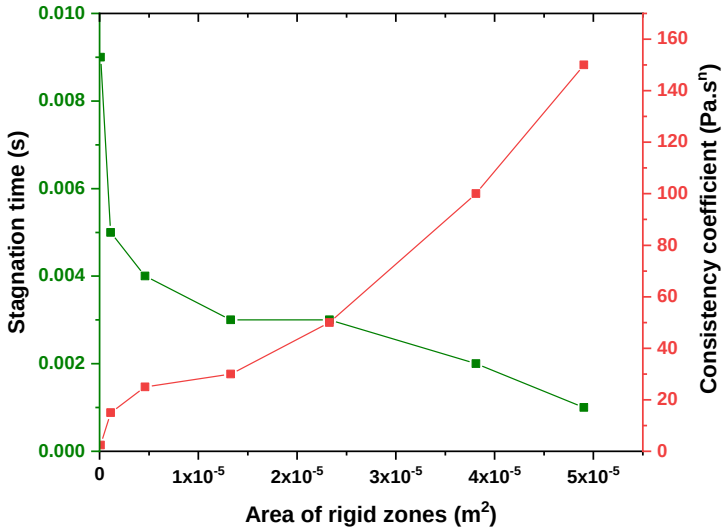

Fig.8. Variation of stagnation time with consistency coefficient in the formation of rigid zones.

The results, illustrated in **Figure 8**, reveal a distinct behavior: as the consistency coefficient increases, the area of the rigid zones expands considerably, while the stagnation time the moment at which these rigid zones stop growing decreases significantly. This trend reflects the fundamental influence of material resistance to deformation on both the spatial and temporal development of rigid zones.

To describe this behavior quantitatively, an empirical model was extracted from the curve, expressing the stagnation time as a function of the rigid zone area. This relationship is given by:

$$t_{\infty} = c(1 + A_{rigid})^{q} \tag{13}$$

where c, q are empirical constants derived from curve fitting. This equation highlights that the evolution of stagnation time is strongly influenced by the extent of solidified zones and allows predictive estimation of flow arrest times based on material parameters.

Journal of Information Systems Engineering and Management
2025, 10(4)
e-ISSN: 2468-4376
https://www.jisem-journal.com/

Research Article

INFLUENCE OF YIELD STRESS AND APPLIED PRESSURE ON THE TEMPORAL EVOLUTION OF RIGID ZONES

To investigate the effect of both yield stress and applied pressure on the evolution of rigid zones, the curves representing the area of these zones as a function of time were analyzed under three different values of yield stress.

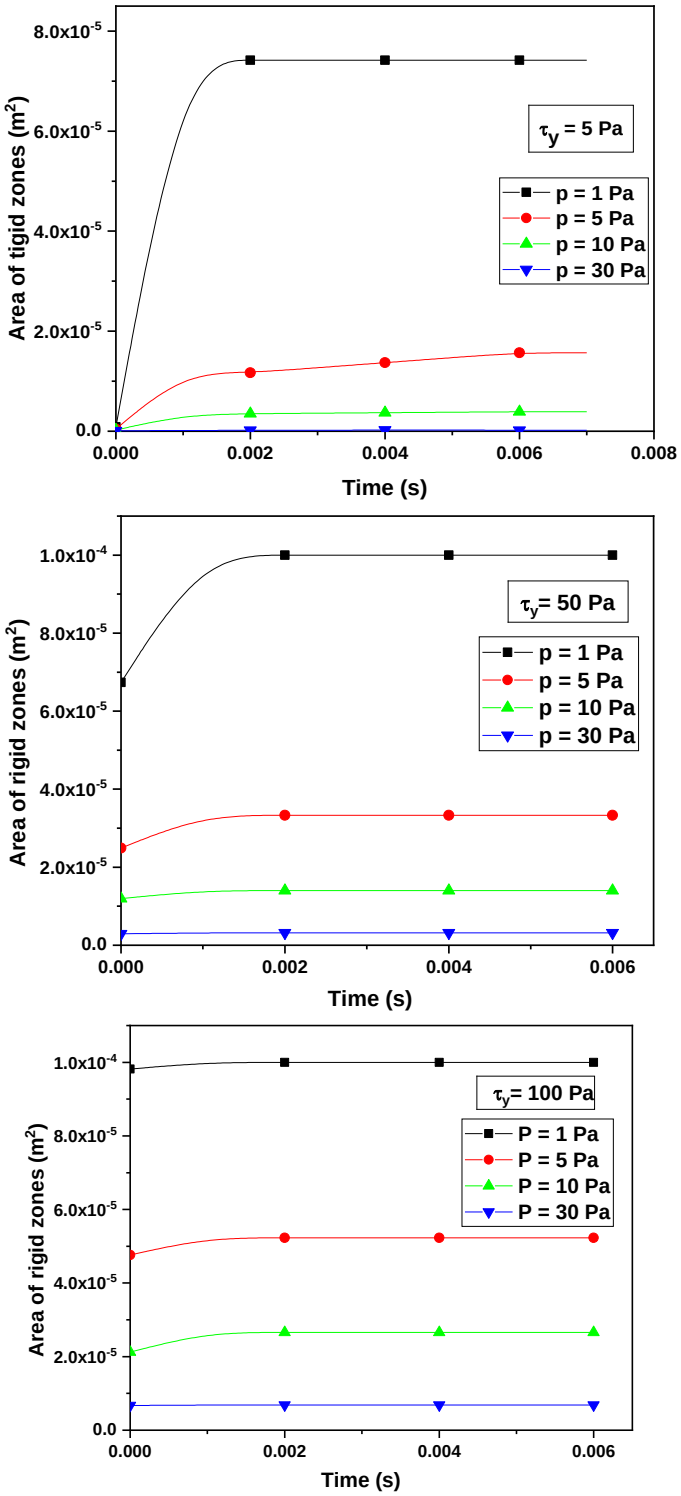

Fig. 9. Evolution of the rigid zone area over time for different pressure values at yield stress $\boldsymbol{\tau_y = 10, 50}$, and $\boldsymbol{100\ Pa}$.

Journal of Information Systems Engineering and Management
2025, 10(4)
e-ISSN: 2468-4376
https://www.jisem-journal.com/

Research Article

Figure 9 clearly demonstrates that the behavior of the concrete significantly varies depending on the values of the yield stress τy and the applied pressure p. For $\tau_y = 5\ Pa$, the rigid zones occupy relatively small areas and exhibit high sensitivity to changes in pressure. It is observed that the largest rigid area forms at the lowest pressure ($p = 1\ Pa$), and it gradually decreases as the pressure increases, almost vanishing at $p = 30\ Pa$. This indicates that at low yield stress, the material is more prone to flow, and even moderate pressures are sufficient to exceed the yield stress throughout most of the domain. At $\tau_y = 50\ Pa$, rigid zones begin to appear more extensively and remain noticeable even at intermediate pressures. However, the same trend is observed again: lower pressure favors the formation of rigid zones, while higher pressure limits their spread. A significant difference arises, however, in that the solidification becomes more resistant to pressure, reflecting a shift in the material's behavior toward greater rigidity. At $\tau_y 100\ Pa$, an almost complete solidification is observed, with large rigid zones persisting even under the highest applied pressure ($p = 30\ Pa$). In this case, the applied pressure is insufficient to generate stress that exceeds the yield threshold in most of the domain, resulting in the formation of wide and stable rigid zones over time.

Based on the curve corresponding to the yield stress threshold of $\tau_y = 50\ Pa$, an empirical equation was derived to estimate the area of rigid zones as a function of time and applied pressure. This curve was chosen for its representative nature, capturing both the transitional and steady-state behavior of the material. The resulting equation provides a practical tool for predicting the rigid zones over time under various pressure conditions.

$$A_{rigid} = z + \frac{G}{\left(1+\left(\frac{t}{D}\right)^{-J}\right)\left(1+\left(\frac{p}{F}\right)^{-M}\right)} \quad (14)$$

Where Z, G, J, F and M are empirical constants derived from curve fitting.

DISCUSSION

Figure 4 explains this phenomenon can be interpreted by recognizing the role of yield stress in resisting deformation. While a low yield stress enables the concrete to flow freely, higher values even once exceeded can hinder the internal flow of the mixture, especially in areas of low local shear. These under-sheared regions act as if they have not fully yielded, forming rigid zones that grow with time due to limited internal mobility and increased cohesion within the material structure.

These results highlight the significant influence of the yield stress parameter in determining whether fresh concrete remains fluid during casting or begins to prematurely solidify. While flow may initiate at a low threshold, increasing the yield stress can reintroduce rigid-like behavior that contradicts the expected fluid performance. Therefore, in both numerical modeling and practical mix design, yield stress must be carefully controlled to prevent unwanted rigid zone formation during flow, ensuring uniform and continuous casting without structural defects or flow blockages.

Complementing this interpretation, **Figure 5** provides spatial insight into how these rigid zones develop and evolve. It reveals that solidification begins with the nucleation of a central rigid nucleus, followed by the emergence of a secondary rigid zone near the inlet. As time progresses, the central nucleus expands and eventually merges with the inlet zone, forming a continuous solidified structure. These spatial observations provide a physical interpretation of the numerical results: the nucleation in the central region and subsequent expansion toward the inlet reflect a dynamic interaction between stress thresholds and local flow resistance. This confirms that yield stress not only governs the quantity of rigid zones, but also controls their spatial distribution and evolution throughout the domain.

Following the insights drawn from the yield stress parameter, attention turns to the role of the consistency coefficient k in shaping the formation and progression of rigid zones. **Figure 6** illustrates this behavior, showing that when k is small, particles remain dispersed and mobile, allowing the mixture to deform easily under shear. However, higher values of k introduce increased internal friction and resistance to flow. Under these conditions, inter-particle forces such as van der Waals attractions and colloidal adhesion begin to dominate, promoting the aggregation of particles into more stable, rigid-like structures.

Journal of Information Systems Engineering and Management
2025, 10(4)
e-ISSN: 2468-4376
https://www.jisem-journal.com/

Research Article

This phenomenon becomes particularly apparent in regions where the shear rate is inherently low such as near the domain boundaries or in the central core of the flow field. In these under-sheared areas, the inability of the applied shear to overcome internal cohesion results in the emergence of persistent rigid zones. As k increases, these zones not only appear earlier but also grow and merge more rapidly, ultimately leading to quasi-complete solidification of the domain at high k values.

These findings align well with the previous discussion of yield stress: both parameters independently and synergistically influence the rheological behavior of fresh concrete during flow. While yield stress dictates the threshold for initiating flow and maintaining deformation, the consistency coefficient governs the ease with which the material continues to deform once flow has started. Together, they shape the temporal and spatial dynamics of rigid zone formation. This interplay emphasizes the importance of carefully selecting both rheological parameters during mix design, as excessive values of either can impede casting performance and result in premature flow stoppage or non-uniform solidification, ultimately compromising the quality of the final structure.

This behavior is further clarified in **Figure 7**, which visually depicts the expansion of rigid zones with increasing consistency coefficient k. The emergence and growth of these zones can be attributed to enhanced particle clustering and internal friction, which inhibit flow and promote microstructural buildup. These rigid networks tend to nucleate in low-shear regions and gradually extend throughout the domain as k increases. This pattern underscores the strong influence of rheology on flow resistance and premature solidification, highlighting the need to balance consistency for effective casting without inducing flow blockages or defects.

This trend is further quantified in **Figure 8**, which highlights the influence of the consistency coefficient on the stagnation time the period required for rigid zones to stabilize.

In highly viscous materials (with larger consistency coefficients), the resistance to shear deformation increases. This enhanced resistance promotes the early formation of rigid zones, as the flow becomes more inhibited. Microscopically, this behavior can be attributed to the interaction and clustering of suspended rigid-like particles. At rest, these particles are randomly oriented in their minimal energy configuration. Under flow, especially when the fluid exhibits high consistency, the particles begin to align or aggregate, resulting in localized solidification. These rigid zones tend to first appear near the walls forming stagnation zones and then extend toward the interior, creating core-like structures. This was previously observed in the contour images where rigid zones emerged both near boundaries and at the center of the domain.

As the consistency increases, these rigid structures form more rapidly, and their growth reaches a steady state in a shorter time. This explains the sharp decrease in stagnation time with higher consistency coefficients. Consequently, not only do rigid zones become more extensive, but they also develop and stabilize much faster, suggesting a strong inverse relationship between fluid mobility and structural resistance.

Moreover, the results shown in **Figure 9** further elucidate the role of applied pressure in conjunction with yield stress in controlling the development and collapse of rigid zones. From a physical standpoint, these results can be interpreted in light of the properties of the Herschel-Bulkley fluid, for which the local stress must exceed the yield stress τ_γ to initiate flow. When the applied pressure is low relative to the yield stress, rigid zones emerge and gradually expand as the flow develops. Initially, solidification grows slowly, then progresses in a pseudo-linear manner with time until reaching a maximum area where it stabilizes. At higher yield stress values, the rigid zones tend to remain stable under low pressure and only begin to shrink when the applied pressure becomes high enough to overcome the yield threshold, as observed when transitioning from $\tau_y = 5\ Pa$ to $\tau_y = 100\ Pa$. This behavior highlights that, when the applied pressure exceeds the yield stress, the Herschel-Bulkley fluid begins to behave similarly to a power-law fluid, wherein the rigid zones completely collapse and the flow becomes more uniform and widespread.

Therefore, the extent of rigid zone breakdown depends on the magnitude of the applied pressure: the higher the pressure, the greater the deformation and the more the rigid zones diminish, enhancing the fluid's capacity to flow. Conversely, higher yield stress values require correspondingly higher pressures to trigger flow initiation. This implies that the interactive relationship between τ_γ and p plays a crucial role in governing the flow behavior and the distribution of rigid zones, underscoring the significant impact of these two parameters in controlling the rheological

behavior of fresh concrete during casting or mold filling.

CONCLUSION

In this numerical investigation, the flow behavior of fresh concrete was studied using the Herschel–Bulkley model with Papanastasiou regularization under unsteady-state conditions within a two-dimensional plate domain. The analysis focused on the development of rigid zones, which appear once the local stress surpasses the yield stress threshold during flow. The study began with a validation step, in which the numerically computed horizontal velocity profile under steady-state conditions was compared against an analytical velocity distribution derived from theoretical formulations. This comparison allowed for an assessment of numerical accuracy. Subsequently, the study examined the effect of yield stress on the temporal evolution of rigid zones. It was found that low yield stress values resulted in minimal or nearly absent solid regions, while higher values led to an earlier onset and more pronounced growth of rigid zones over time. At sufficiently high yield stress levels, complete solidification of the domain was observed. A mathematical expression was derived to predict the rigid zone area as a function of yield stress and time, providing a quantitative basis for anticipating the onset and progression of solidification during flow. The investigation further revealed that increasing the consistency index results in a noticeable expansion of these rigid zones. A separate mathematical relationship was formulated to predict the rigid zone area as a function of the consistency index. Additionally, an expression was developed to determine the stagnation time defined as the moment when the rigid zone area reaches a steady state based on both the consistency index and the rigid area. The effect of applied pressure on the temporal evolution of rigid zones was also explored across different yield stress values. It was observed that lower pressure levels favor the persistence of rigid zones, whereas higher pressures promote a transition toward power-law fluid behavior, thereby diminishing solidification. For a representative scenario with a yield stress of 50 Pa, a mathematical correlation was derived to estimate the rigid zone area as a function of both pressure and time.

To ensure accurate and physically consistent outcomes, this study underscores the necessity of carefully tuning the rheological parameters and boundary conditions. The derived predictive expressions offer valuable tools for quantifying the spatial and temporal evolution of rigid zones, contributing to enhanced control strategies in concrete casting processes and other applications involving viscoplastic fluids.

REFRENCES

[1] R. P. Chhabra, Non-Newtonian fluids: An introduction, in Rheology of Complex Fluids, edited by J. Krishnan, A. Deshpande, and P. Kumar (Springer, New York, NY, 2010), Chap. 1.
[2] R. P. Chhabra, J.F. Richardson, Non-Newtonian flow and applied rheology.2nd edn. Butterworth-Heinemann, Oxford, (2008).
[3] A. Paiva, F. Petronetto, T. Lewiner, G. Tavares, Particle-based viscoplastic fluid/ri simulation. 41 (2009) 306-314.
[4] K. Vajravelu, S. Sreenadh, V. Ramesh Babu, Peristaltic pumping of a Herschel–Bulkley fluid in a Channel. 169 (2005) 726-35.
[5] C. Ancey, S. Cochard, The dam-break problem for Herschel-Bulkley viscoplastic fluids down steep flumes. J. Non-Newton. Fluid Mech. 158(1–3), 18-35 (2009).
[6] N. J. Balmforth, A.S. Burbidge, R.V. Craster, J. Salzig and A. Shen, Visco-plastic models of isothermal lava domes. J. Fluid Mech. 403, 37-65 (2000).
[7] T.C. Papanastasiou, Flows of Materials with Yield. J. Rheol. 31, 385-404 (1987).
[8] C. Mai Bui, T. Xuan Ho, Numerical study of an unsteady flow of thixotropic liquids past a cylinder. AIP Advances. 9, 115002 (2019).
[9] E. Mitsoul W, S. S. Abdali, flow simulation of herschel-bulkley fluids through extrusion dies.the canadian journal of chemical engineering. 71, (1993).
[10] S. Nallapu, G. Radhakrishnamacharya, ali j. Chamkha, effect of slip on herschel–bulkley fluid flow through narrow tubes, alexandria eng. J. 54 (2015) 889-896.
[11] S. Mossaz, P. Jay, A. Magnin, Criteria for the appearance of recirculating and non-stationary regimes behind a cylinder in a viscoplastic fluid, J. Non-Newtonian Fluid Mech. 165 (2010) 1525– 1535.

Research Article

[12]S. Mossaz, P. Jay, and A. Magnin, Non-recirculating and recirculating inertial flows of a viscoplastic fluid around a cylinder, J. Non-Newtonian Fluid Mech. 64–75 (2012) 177-178.
[13] D.L. Tokpavi, A. Magnin, P. Jay, Very slow flow of Bingham viscoplastic fluid around a circular cylinder, J. Non-Newtonian Fluid Mech. 154 (2008) 65–76.
[14]F. Messelmi, Effects of the yield limit on the behavior of Herschel-Bulkley fluid, Nonlinear Sci. Lett. A 2 (3) (2011) 137-142.
[15] H. Taibi, F. Messelmi, Effect of yield stress on the behavior of rigid zones during the laminar flow of Herschel-Bulkley fluid, Alexandria Eng. J.57(2017)1109-1115.
[16] P. Saramito, A new elastoviscoplastic model based on the Herschel-Bulkley viscoplastic model. Journal of Non-Newtonian Fluid Mechanics, Elsevier.158 (1-3), (2009) 154-161.
[17] E. Moreno, A. Larese, M. Cervera, Modelling of Bingham and Herschel–Bulkley flows with mixed P1/P1 finite elements stabilized with orthogonal subgrid scale. J. Non-Newtonian Fluid. Mech.228 (2016) 1-16.
[18] R.B. Spelay, Solids Transport in Laminar, Open Channel Flow of Non-Newtonian Slurries Ph. D. thesis, Chemical Engineering Dept., University of Saskatchewan, Saskatoon, Saskatchewan, 2007.
[19] E. Mitsoulis, Flows of viscoplastic materials: models and computations, Rheol. Rev. (2007) 135– 178.
[20] J.D. Dent, T.E. Lang, A Biviscous modified Bingham model of snow avalanche motion, Ann. Glaciol. 4 (1983).
[21] H. Zhu, Y.D. Kim, D. Dekee, Non-Newtonian fluids with a yield stress, J. Non-Newtonian Fluid Mech. 129 (2005) 177–181.
[22] E. Moreno, y.M. Cervera, Elementos finitos mixtos estabilizados para flujos confinados de Bingham y de Herschel-Bulkley. Parte I: Formulación. Rev. int. métodos numér. cálc. diseño ing. (2016) 32(2) 100-109.
[23] M. Thiedeitz, T. Kränkel, D. Kartal, J. J. Timothy, “The slump flow of cementitious pastes: Simulation vs. experiments,” Materials. (2024) 17(2), 532.
[24] J. Bleyer, M. Maillard, P. Buhan, P. Coussot, “Efficient numerical computations of yield stress fluid flows using second-order cone programming,” Comput. Methods Appl. Mech. Engrg. 283 (2015) 599–614.